

Constituent Automorphism Decoding of Reed–Muller Codes

Yicheng Qu, Amir Tasbihi, and Frank R. Kschischang

Abstract—Automorphism-ensemble decoding is applied to the Plotkin constituents of Reed–Muller codes, resulting in a new soft-decision decoding algorithm with state-of-the-art performance versus complexity trade-offs.

Index Terms—Reed–Muller codes, automorphism ensemble decoding, successive cancellation list decoding.

I. INTRODUCTION

THIS paper introduces the *constituent automorphism* (CA) decoder, a new soft-decision decoding algorithm for Reed–Muller (RM) codes. The new algorithm, a variant of automorphism ensemble (AE) decoding [1], exploits the recursive Plotkin structure of RM codes, applying AE decoding to constituent RM codes located at various levels in the resulting decoding tree. By carefully adjusting the number of automorphisms applied to particular constituent decoders, CA decoding results in better performance versus complexity trade-offs than other state-of-the-art decoding algorithms such as successive cancellation list (SCL) decoding [2] and AE decoding itself [1] (where automorphisms are applied only at the root of the decoding tree).

Although Reed–Muller codes are among the earliest families of codes introduced in coding theory [3], [4], contemporary interest in them arises from (a) their excellent soft-decision decoding performance at short block lengths, (b) their close connection to polar codes, (c) the relatively recent discovery that RM codes can be capacity-achieving in certain situations, and (d) the fact that RM codes arise in connection with various problems in theoretical computer science; see [5] for an excellent review. In [6], Schnabl and Bossert view RM codes as generalized multiple concatenated (GMC) codes, introducing the first soft-decision RM decoding algorithm—herein referred to as the GMC decoder—by exploiting their recursive Plotkin structure to successively decode their constituent codes. In the literature on polar codes [7], the GMC decoder is also often referred to as a *successive cancellation* (SC) decoder. In [2], Dumer and Shabunov show that better RM soft-decision decoding performance can be obtained for the binary-input additive white Gaussian noise (BI-AWGN) channel by combining GMC decoding with list-decoding. The resulting successive-cancellation list (SCL) decoder was extended to polar codes in [8].

The idea of exploiting code automorphisms for decoding dates back to the 1960s [9], [10]. Recent interest in automorphism-based decoders for RM codes [1], [11], [12] stems from their ability to approach maximum-likelihood (ML) decoding performance with a reasonable complexity. The general idea is to permute the received vector by the elements of a set \mathcal{E} of code automorphisms, then to decode the permuted versions in parallel via a simple sub-optimal *elementary decoder*. The inverse automorphism is then applied to each decoded word to arrive at a list of $|\mathcal{E}|$ (not necessarily distinct) decoding candidates, where $|\mathcal{E}|$ denotes the number of elements in \mathcal{E} . The decoder then selects the most likely codeword from the candidate list. While the automorphism-based decoder is approximately $|\mathcal{E}|$ times computationally more complex than its elementary decoder, its inherent parallelism makes it very hardware-friendly [13], which may be seen as an advantage of AE decoding compared with SCL decoding. The key idea of this paper is to apply AE decoding at the level of the Plotkin constituent codes of a Reed–Muller code. This maintains a high degree of parallelism in the decoding algorithm and, as we demonstrate, it can result in performance-complexity benefits.

The remainder of this paper is organized as follows. Various coding-theoretic preliminaries needed to understand the rest of the paper are reviewed in Sec. II. The CA decoder is introduced in Sec. III, and its complexity is analyzed in Sec. IV. Simulation results showing performance and complexity tradeoffs are given in Sec. V, along with comparisons to other state-of-the-art RM decoders. Some brief concluding remarks are given in Sec. VI.

Throughout this paper, the real numbers are denoted by \mathbb{R} , the integers are denoted by \mathbb{Z} , and the two-element finite field $\{0, 1\}$ is denoted by \mathbb{F}_2 . The extended real numbers $\mathbb{R} \cup \{-\infty, +\infty\}$ are denoted as $\bar{\mathbb{R}}$. The (modulo-two) addition operation in \mathbb{F}_2 , equivalent to an exclusive-OR (XOR) operation, is denoted as \oplus . The *soft XOR* of two extended real numbers $a, b \in \bar{\mathbb{R}}$, denoted as $a \boxplus b$, is given as

$$a \boxplus b \triangleq 2 \tanh^{-1} \left(\tanh \left(\frac{a}{2} \right) \tanh \left(\frac{b}{2} \right) \right),$$

where $\tanh(\pm\infty) = \pm 1$, and where the symbol ‘ \triangleq ’ signifies that the right-hand side is the definition of the left-hand side. The *negative log-sigmoid* of $x \in \bar{\mathbb{R}}$ is given as

$$\eta(x) \triangleq \ln(1 + \exp(-x)), \quad (1)$$

where $\eta(-\infty) = \infty$ and $\eta(\infty) = 0$. For any integer k ,

$$\mathbb{Z}^{\geq k} \triangleq \{k, k+1, \dots\} \text{ and } \mathbb{Z}^{\leq k} \triangleq \{\dots, k-1, k\}.$$

The authors are with the Edward S. Rogers Sr. Dept. of Electrical and Computer Engineering, University of Toronto, 10 King’s College Road, Toronto, Ontario M5S 3G4, Canada. Email: eason.qu@mail.utoronto.ca, amir.tasbihi@mail.utoronto.ca, frank@ece.utoronto.ca. Submitted for publication on July 19th, 2024.

For any $n \in \mathbb{Z}^{\geq 0}$, $[n] \triangleq \{0, 1, \dots, n-1\}$, where $[0]$ is the empty set. The mapping $(-1)^{(\cdot)} : \mathbb{F}_2 \rightarrow \mathbb{R}$ is defined, for $b \in \mathbb{F}_2$, as

$$(-1)^b \triangleq \begin{cases} 1, & \text{if } b = 0; \\ -1, & \text{if } b = 1. \end{cases}$$

For any predicate p , $\mathbb{1}_p$ denotes the indicator function

$$\mathbb{1}_p \triangleq \begin{cases} 1, & \text{if } p \text{ is true;} \\ 0, & \text{otherwise.} \end{cases}$$

The codomain of $\mathbb{1}_p$ may be $\overline{\mathbb{R}}$ or \mathbb{F}_2 as context dictates. Vectors (over $\overline{\mathbb{R}}$ or \mathbb{F}_2) are denoted with boldface lowercase letters. A vector of length n , *i.e.*, a vector having n components, is referred to as an n -vector. The i th component of an n -vector \mathbf{v} is denoted $\mathbf{v}[i]$, where $i \in [n]$. The empty vector $\emptyset \triangleq ()$ has zero length and no components. The *concatenation* of an n_1 -vector \mathbf{u} and an n_2 -vector \mathbf{v} , in that order, is the $(n_1 + n_2)$ -vector

$$(\mathbf{u} \mid \mathbf{v}) \triangleq (\mathbf{u}[0], \dots, \mathbf{u}[n_1 - 1], \mathbf{v}[0], \dots, \mathbf{v}[n_2 - 1]).$$

Generally $(\mathbf{u} \mid \mathbf{v}) \neq (\mathbf{v} \mid \mathbf{u})$, although $(\mathbf{u} \mid \emptyset) = (\emptyset \mid \mathbf{u}) = \mathbf{u}$. The all-zero and all-one n -vectors over \mathbb{F}_2 are denoted as $\mathbf{0}_n$ and $\mathbf{1}_n$, respectively, where the subscript may be omitted if the length is clear from the context. For any binary vector \mathbf{b} and any real vector $\boldsymbol{\lambda}$ of the same length, $(-1)^{\mathbf{b}}\boldsymbol{\lambda}$ denotes a real vector whose i th component is $(-1)^{\mathbf{b}[i]}\boldsymbol{\lambda}[i]$. For any $n \in \mathbb{Z}^{\geq 0}$, $((a_i, b_i)_{i \in [n]})$ denotes the n -tuple of 2-tuples $((a_0, b_0), (a_1, b_1), \dots, (a_{n-1}, b_{n-1}))$, where the a_i 's and b_i 's are arbitrary mathematical objects. This notation may be generalized to n -tuples of m -tuples in the obvious way. For any $m \in \mathbb{Z}^{\geq 0}$, the ring of m -variate binary polynomials with indeterminates x_0, \dots, x_{m-1} is denoted by $\mathbb{F}_2[x_0, \dots, x_{m-1}]$. When $m = 0$ we have $\mathbb{F}_2[] \triangleq \mathbb{F}_2$. For any $r \in \mathbb{Z}$, $\mathbb{F}_2^{\leq r}[x_0, \dots, x_{m-1}]$ denotes the set of polynomials in $\mathbb{F}_2[x_0, \dots, x_{m-1}]$ whose total degree is at most r . The total degree of the zero polynomial 0 is taken as $-\infty$; thus for any $r < 0$, $\mathbb{F}_2^{\leq r}[x_0, \dots, x_{m-1}] = \{0\}$.

II. PRELIMINARIES

In this section we briefly review various coding-theoretic concepts needed to understand the remainder of the paper.

A. Channels and Decoders

Throughout this paper, we assume the use of a binary-input memoryless channel with input alphabet \mathbb{F}_2 , output alphabet \mathcal{Y} , and channel law given, for $x \in \mathbb{F}_2$ and $y \in \mathcal{Y}$, as $W(y \mid x)$, where W is either a conditional probability mass function or conditional probability density function according to whether \mathcal{Y} is discrete or continuous. Without loss of generality, we assume that \mathcal{Y} is chosen so that $W(y \mid 0) \neq 0$ or $W(y \mid 1) \neq 0$ for all $y \in \mathcal{Y}$.

A standard example of such a channel is the binary symmetric channel with crossover probability p , where $\mathcal{Y} = \mathbb{F}_2$ and $W(1 \mid 0) = W(0 \mid 1) = p$. Another example is the binary erasure channel (BEC) with erasure probability ϵ , where $\mathcal{Y} = \mathbb{F}_2 \cup \{e\}$ and $W(e \mid 0) = W(e \mid 1) = \epsilon$ and

$W(0 \mid 1) = W(1 \mid 0) = 0$. Another standard example, and the one we use to present simulation results, is the BI-AWGN with noise variance σ^2 , where $\mathcal{Y} = \mathbb{R}$, with $W(y \mid 0) = \mathcal{N}(1, \sigma^2)$ and $W(y \mid 1) = \mathcal{N}(-1, \sigma^2)$, where $\mathcal{N}(m, \sigma^2)$ denotes a Gaussian density function with parameters m and σ^2 . The signal-to-noise ratio (SNR) of such a channel is $1/\sigma^2$.

Associated with each received channel output $y \in \mathcal{Y}$ is the log-likelihood ratio (LLR) $\Lambda(y) \triangleq \ln \left(\frac{W(y \mid 0)}{W(y \mid 1)} \right) \in \overline{\mathbb{R}}$, where $\Lambda(y) = -\infty$ if $W(y \mid 0) = 0$ and $\Lambda(y) = +\infty$ if $W(y \mid 1) = 0$. Infinite LLRs occur, for example, for unerased symbols received at the output of the BEC. The *hard decision* associated with an LLR value $\lambda = \Lambda(y)$, for some channel output y , is given by the function $b : \overline{\mathbb{R}} \rightarrow \mathbb{F}_2$, where $b(\lambda) \triangleq \mathbb{1}_{\lambda < 0}$.

Suppose that a binary codeword of length n is transmitted. Based on the corresponding channel output $\mathbf{y} \in \mathcal{Y}^n$, we assume that the receiver produces the log-likelihood-ratio (LLR) vector $\boldsymbol{\lambda} \in \overline{\mathbb{R}}^n$, where $\boldsymbol{\lambda}[i] = \Lambda(\mathbf{y}[i])$ for $i \in [n]$. The LLR vector serves as the interface between the channel and the decoder. We also define the vector of hard-decisions $\mathbf{b}(\boldsymbol{\lambda}) \in \mathbb{F}_2^n$ as a binary n -vector whose entries are hard decisions associated with $\boldsymbol{\lambda}$ entries, *i.e.*, $\mathbf{b}(\boldsymbol{\lambda})[i] \triangleq \mathbf{b}(\boldsymbol{\lambda}[i])$ for $i \in [n]$.

A *decoding rule* or simply *decoder* for a binary code C of length n is a function $D : \overline{\mathbb{R}}^n \rightarrow C \cup \{F\}$ that maps an LLR vector $\boldsymbol{\lambda}$ either to a codeword of C or to the symbol F (which indicates a decoding failure). Two decoders D_1 and D_2 are *the same* for a given channel if they almost surely produce the same decoding decision, *i.e.*, if $\Pr(D_1(\boldsymbol{\lambda}) \neq D_2(\boldsymbol{\lambda})) = 0$, where $\boldsymbol{\lambda}$ is the LLR vector corresponding to the channel output. We write $D_1 \neq D_2$ when D_1 and D_2 are not the same.

The *analog weight* $w(\mathbf{x}, \boldsymbol{\lambda})$ of a channel input \mathbf{x} with respect to an LLR vector $\boldsymbol{\lambda}$ is given as the sum of the absolute values of those components of $\boldsymbol{\lambda}$ whose hard-decisions disagree with the corresponding component of \mathbf{x} , *i.e.*,

$$w(\mathbf{x}, \boldsymbol{\lambda}) \triangleq \sum_{i: \mathbf{x}[i] \neq \mathbf{b}(\boldsymbol{\lambda}[i])} |\boldsymbol{\lambda}[i]|. \quad (2)$$

The analog weight $w(\mathbf{x}, \boldsymbol{\lambda})$ measures the cost of disagreements between \mathbf{x} and $\mathbf{b}(\boldsymbol{\lambda})$. Among all possible channel inputs, the hard-decision vector $\mathbf{b}(\boldsymbol{\lambda})$ itself has minimum possible analog weight, namely 0; however, $\mathbf{b}(\boldsymbol{\lambda})$ may not be a codeword. Given an LLR vector $\boldsymbol{\lambda}$, a *maximum-likelihood (ML) decoder* for a code C produces a codeword $\mathbf{v} \in C$ having least analog weight with respect to $\boldsymbol{\lambda}$. If codewords are equally likely to be transmitted, an ML decoder minimizes block error rate (BLER), *i.e.*, the probability that the decoding decision disagrees with the transmitted codeword.

B. Code Automorphisms

For any positive integer n , a *permutation* of order n is a bijection $\pi : [n] \rightarrow [n]$. The set of all permutations of order n forms a group (the *symmetric group* S_n) under function composition. The group identity is denoted as *id*. The symmetric group S_n acts on n -vectors by permutation of coordinates, *i.e.*, for any n -vector \mathbf{v} and any $\pi \in S_n$,

$$\pi \mathbf{v} \triangleq (\mathbf{v}[\pi(0)], \dots, \mathbf{v}[\pi(n-1)]).$$

A permutation $\pi \in S_n$ is called an *automorphism* of a code C of length n if $\mathbf{c} \in C$ implies $\pi\mathbf{c} \in C$. In other words, an automorphism of a code is a permutation which maps codewords to codewords. The set of all automorphisms of C form a subgroup of S_n called the *automorphism group* of C .

C. Reed–Muller Codes

Fix $m \in \mathbb{Z}^{\geq 0}$. For any polynomial $p = p(x_0, \dots, x_{m-1}) \in \mathbb{F}_2[x_0, \dots, x_{m-1}]$, and any binary m -vector \mathbf{v} , called a *point*, let $p(\mathbf{v}) = p(\mathbf{v}[0], \dots, \mathbf{v}[m-1]) \in \mathbb{F}_2$ denote the *evaluation* of the polynomial p at the point \mathbf{v} , *i.e.*, the binary value obtained when x_i is substituted with $\mathbf{v}[i]$, for each $i \in [m]$. When $m = 0$, we have $p(\emptyset) = 0$ if $p = 0$ and $p(\emptyset) = 1$ if $p = 1$. Define the *evaluation map* $\text{eval} : \mathbb{F}_2[x_0, \dots, x_{m-1}] \rightarrow \mathbb{F}_2^{2^m}$ as the function which maps the polynomial $p \in \mathbb{F}_2[x_0, \dots, x_{m-1}]$ to its evaluation at *all* points of \mathbb{F}_2^m in lexicographic order, *i.e.*,

$$\text{eval}(p) \triangleq \left(p(0, \dots, 0, 0), p(0, \dots, 0, 1), p(0, \dots, 1, 0), \dots, p(1, \dots, 1, 1) \right). \quad (3)$$

For any $r \in \mathbb{Z}$ and any $m \in \mathbb{Z}^{\geq 0}$, the binary Reed–Muller code of *log-length* m and *order* r , denoted as $\text{RM}(r, m)$, is the image of $\mathbb{F}_2^{\leq r}[x_0, \dots, x_{m-1}]$ under the evaluation map, *i.e.*,

$$\text{RM}(r, m) \triangleq \left\{ \text{eval}(p) : p \in \mathbb{F}_2^{\leq r}[x_0, \dots, x_{m-1}] \right\}. \quad (4)$$

It can be shown (see, *e.g.*, [14, Fig. 13.4]), for any $m \in \mathbb{Z}^{\geq 0}$ and any integer r satisfying $0 \leq r \leq m$, that $\text{RM}(r, m)$ is a code of block length $n = 2^m$, dimension

$$k(r, m) \triangleq \sum_{i=0}^r \binom{m}{i}$$

and minimum Hamming distance $d = 2^{m-r}$. When $r < 0$, $\text{RM}(r, m) = \{\mathbf{0}_{2^m}\}$ contains only the zero codeword. When $r = 0$, $\text{RM}(r, m)$ is the binary repetition code of length 2^m . When $r = m - 1$, $\text{RM}(m - 1, m)$ is the $(2^m, 2^m - 1)$ single-parity check (SPC) code. When $r \geq m$, $\text{RM}(r, m) = \mathbb{F}_2^{2^m}$ (the whole space of 2^m -vectors). These are the *trivial* RM codes. When $0 < r < m - 1$, we call $\text{RM}(r, m)$ *nontrivial*.

RM codes are one of the few algebraic code families with a well-characterized automorphism group. We denote the automorphism group of $\text{RM}(r, m)$ by $\mathbb{A}_{r,m}$. When $\text{RM}(r, m)$ is nontrivial, it is known [5] [14, Sec. 13.9] that $\mathbb{A}_{r,m}$ is isomorphic to the general affine group $\text{GA}(m, \mathbb{F}_2)$. When $\text{RM}(r, m)$ is trivial, $\mathbb{A}_{r,m}$ is equal to S_{2^m} (*i.e.*, every permutation of coordinates is an automorphism).

Under the lexicographic order by which the evaluation map in (3) is defined, one may show that RM codes admit a Plotkin structure [15]. This means that any codeword $\mathbf{c} \in \text{RM}(r, m)$, where $m \geq 1$, can be written as

$$\mathbf{c} = (\mathbf{u} \mid \mathbf{u} \oplus \mathbf{v}),$$

where $\mathbf{u} \in \text{RM}(r, m - 1)$ and $\mathbf{v} \in \text{RM}(r - 1, m - 1)$. We refer to $\text{RM}(r, m - 1)$ and $\text{RM}(r - 1, m - 1)$ as the

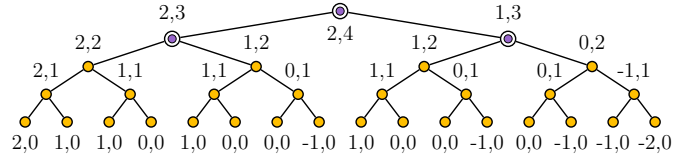


Fig. 1. Illustrated is $\mathbb{T}_{2,4}$. The label of each vertex is (r, m) , for some $r \in \mathbb{Z}$ and $m \in \mathbb{Z}^{\geq 0}$, where for brevity the parentheses are omitted. The circled vertices form $\mathbb{T}_{2,4}^{A^*}$, the GMC decoding tree for $\text{RM}(2, 4)$ with atom set A^* in (8).

Plotkin constituents of $\text{RM}(r, m)$. Of course $\text{RM}(r, m - 1)$ and $\text{RM}(r - 1, m - 1)$ are themselves RM codes, having their own Plotkin constituents.

The relationships among the various Plotkin constituents of $\text{RM}(r, m)$ are readily visualized using a binary tree, called a *Plotkin tree*, and denoted $\mathbb{T}_{r,m}$. Each vertex in the tree is labelled with a pair of integers (r', m') ; in particular, the root is labelled with (r, m) . A vertex v with label (r', m') where $m' > 0$ has two children: the left child has label $(r', m' - 1)$ and the right child has label $(r' - 1, m' - 1)$. Vertices (r', m') with $m' = 0$ are leaf vertices; they have no children. Fig. 1 illustrates $\mathbb{T}_{2,4}$.

Since it is possible for some vertices in $\mathbb{T}_{r,m}$ to have the same label, it is useful to assign a unique variable-length binary *address* to each vertex. The construction is standard: the root is assigned address \emptyset , and throughout the tree (or any rooted subtree thereof), the left child of a vertex with the address \mathbf{a} receives address $(\mathbf{a} \mid 0)$, while the right child receives address $(\mathbf{a} \mid 1)$. However, rather than writing addresses as vectors, we will write them as binary strings. For example, Fig. 2 illustrates the vertex addresses for a rooted subtree of $\mathbb{T}_{3,6}$. If the root of the tree has label (r, m) , then a vertex with address \mathbf{a} has label $(r - \text{wt}(\mathbf{a}), m - \text{len}(\mathbf{a}))$, where $\text{wt}(\mathbf{a})$ denotes the Hamming weight of \mathbf{a} and $\text{len}(\mathbf{a})$ denotes the length of \mathbf{a} .

In principle, soft-decision ML decoding of $\text{RM}(r, m)$ can be accomplished via the Viterbi algorithm; however the number of edges in the trellis diagram scales at least exponentially in the block length [16, Sec. IV.A], making this approach computationally infeasible for all but very short RM codes. On the other hand, ML decoding of the trivial RM codes (which include repetition codes and SPC codes) is easy. ML decoding of $\text{RM}(m - 1, m)$, the SPC code, is straightforward via the *Wagner* decoding rule [17], with the main complexity being determination of the position in the received word having the smallest LLR magnitude. Soft-decision decoding of first-order RM codes $\text{RM}(1, m)$ can be accomplished using the “Green Machine” decoder [14, Ch. 14] [18], with the main complexity being the computation of a Hadamard transform of the received LLR vector. In the following sections, we discuss some of the non-ML soft-decision decoding algorithms for general RM codes.

D. GMC Decoding of RM Codes

As already noted, the GMC decoder [6] uses a divide-and-conquer approach that exploits the recursive Plotkin structure

of RM codes, splitting the task of decoding $\text{RM}(r, m)$ into that of decoding its Plotkin constituents, namely $\text{RM}(r-1, m-1)$ and $\text{RM}(r, m-1)$. In turn, these smaller decoding problems can themselves be split into even smaller decoding problems, until eventually an “easy” decoding problem is reached, at which point no further task-splitting is required.

To make this precise, let \mathcal{A} , called an *atom set*, be any collection of RM codes for which task-splitting is not required due to the availability of computationally feasible decoders for those codes. For example, \mathcal{A} might contain all trivial RM codes and the first-order RM codes $\text{RM}(1, m)$. We will assume that an atom set always contains trivial RM codes $\text{RM}(r, 0)$ of length 1. An RM code *not* contained in \mathcal{A} is called *composite* with respect to \mathcal{A} . The decoding function for an RM code $\text{RM}(r, m) \in \mathcal{A}$ is denoted as $A_{r,m}$.

Let $\boldsymbol{\lambda} \in \overline{\mathbb{R}}^{2^m}$, denote the LLR vector produced at the output of a binary-input memoryless channel when a codeword of $\text{RM}(r, m)$ is transmitted. The GMC decoder with atom set \mathcal{A} is the function $\Gamma_{r,m}^{\mathcal{A}} : \overline{\mathbb{R}}^{2^m} \rightarrow \text{RM}(r, m)$ recursively defined by

$$\Gamma_{r,m}^{\mathcal{A}}(\boldsymbol{\lambda}) \triangleq \begin{cases} A_{r,m}(\boldsymbol{\lambda}), & \text{if } \text{RM}(r, m) \in \mathcal{A}; \\ (\mathbf{u} \mid \mathbf{u} \oplus \mathbf{v}), & \text{otherwise,} \end{cases} \quad (5)$$

where, assuming $\boldsymbol{\lambda}$ is partitioned as $\boldsymbol{\lambda} = (\boldsymbol{\lambda}' \mid \boldsymbol{\lambda}'')$ with $\boldsymbol{\lambda}', \boldsymbol{\lambda}'' \in \overline{\mathbb{R}}^{2^{m-1}}$, the binary 2^{m-1} -vectors \mathbf{v} and \mathbf{u} are given as

$$\mathbf{v} = \Gamma_{r-1,m-1}^{\mathcal{A}}(\boldsymbol{\lambda}' \boxplus \boldsymbol{\lambda}''), \quad (6)$$

$$\mathbf{u} = \Gamma_{r,m-1}^{\mathcal{A}}(\boldsymbol{\lambda}' + (-1)^{\mathbf{v}} \boldsymbol{\lambda}''), \quad (7)$$

respectively. Since \mathcal{A} is required to include trivial length-1 RM codes, the GMC decoder is guaranteed to terminate.

Note that computation of \mathbf{u} in (7) depends on the availability of \mathbf{v} defined in (6), and both \mathbf{u} and \mathbf{v} are required in (5). In effect, the GMC decoder $\Gamma_{r,m}^{\mathcal{A}}$ performs a reverse post-order traversal of a rooted subtree of $\mathbb{T}_{r,m}$ —called the *GMC decoding tree* with respect to \mathcal{A} and denoted as $\mathbb{T}_{r,m}^{\mathcal{A}}$ —in which vertices with labels corresponding to codes that are composite with respect to \mathcal{A} are internal, and those with labels corresponding to elements of \mathcal{A} are leaves. We refer to the decoders for elements of \mathcal{A} as *leaf decoders*.

The smallest possible atom set contains only the RM codes of length 1, in which case the GMC decoding tree for $\text{RM}(r, m)$ is the same as the Plotkin tree $\mathbb{T}_{r,m}$. However, as noted earlier, another choice for the atom set is the one containing the trivial and the first-order RM codes, *i.e.*,

$$\mathcal{A}^* = \{\text{RM}(r, m) : m \in \mathbb{Z}^{\geq 0}, r \in \mathbb{Z}^{\leq 1} \cup \mathbb{Z}^{\geq m-1}\}. \quad (8)$$

The circled vertices in Fig. 1 illustrate $\mathbb{T}_{2,4}^{\mathcal{A}^*}$, the GMC decoding tree for $\text{RM}(2, 4)$ with atom set \mathcal{A}^* , and Fig. 2 shows the GMC decoding tree $\mathbb{T}_{3,6}^{\mathcal{A}^*}$ (along with the address of each vertex).

It is important to note that GMC decoding, though computationally convenient, does not always return an ML codeword, and therefore GMC decoding does not generally have the smallest possible BLER. The complexity of GMC decoding of an RM code of length n is $\mathcal{O}(n \log n)$ [6], [19]. Because of

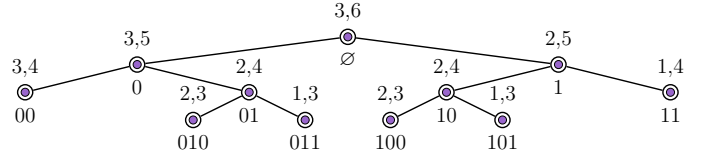


Fig. 2. The address of each vertex in $\mathbb{T}_{3,6}^{\mathcal{A}^*}$ is indicated below that vertex; the vertex label is indicated above.

its low complexity (and its suboptimality), the GMC decoder can be used as an elementary decoder in AE decoding; see Sec. II-F.

E. SCL Decoding of RM Codes

SCL decoders generalize GMC decoders by allowing the constituent decoders to return not just a single codeword, but rather a *list* of possible codewords. In SCL decoding, the atom set is usually chosen as $\mathcal{A}' \triangleq \{\text{RM}(r, 0) : r \in \mathbb{Z}\}$, which contain only RM codes of length 1. To avoid an exponential growth of the decoding list, an upper bound on the returned list size at each constituent decoder is maintained, retaining only those candidate codewords of lowest *cost*, defined as follows [20]. For any LLR vector $\boldsymbol{\lambda} \in \overline{\mathbb{R}}^{2^m}$ and any $\mathbf{c} \in \text{RM}(r, m)$, let

$$\mathcal{L}(\mathbf{c}, \boldsymbol{\lambda}) \triangleq \sum_{i \in [2^m]} \eta \left((-1)^{c[i]} \lambda[i] \right) \quad (9)$$

be the cost of decoding the LLR vector $\boldsymbol{\lambda}$ to the vector \mathbf{c} , where η was defined in (1). If $\boldsymbol{\lambda} = (\boldsymbol{\lambda}' \mid \boldsymbol{\lambda}'')$, for some $\boldsymbol{\lambda}'$ and $\boldsymbol{\lambda}'' \in \overline{\mathbb{R}}^{2^{m-1}}$, and if $\mathbf{c} = (\mathbf{u} \mid \mathbf{u} \oplus \mathbf{v})$, then

$$\mathcal{L}(\mathbf{c}, \boldsymbol{\lambda}) = \mathcal{L}(\mathbf{v}, \boldsymbol{\lambda}' \boxplus \boldsymbol{\lambda}'') + \mathcal{L}(\mathbf{u}, \boldsymbol{\lambda}' + (-1)^{\mathbf{v}} \boldsymbol{\lambda}''). \quad (10)$$

The terms $\mathcal{L}(\mathbf{v}, \boldsymbol{\lambda}' \boxplus \boldsymbol{\lambda}'')$ and $\mathcal{L}(\mathbf{u}, \boldsymbol{\lambda}' + (-1)^{\mathbf{v}} \boldsymbol{\lambda}'')$ may be regarded as the *Plotkin constituent costs* of $\mathbf{c} = (\mathbf{u} \mid \mathbf{u} \oplus \mathbf{v})$; the SCL decoder exploits this additive decomposition of the overall cost of \mathbf{c} .

SCL decoding proceeds recursively in the same manner as the GMC decoder, except, rather than being provided with a single LLR vector, the constituent decoders are provided with a list of one or more ordered pairs, where each pair comprises an LLR vector and an associated cost. The output of each constituent decoder is a list of triples, where each triple comprises a codeword, the index within the input list of the LLR vector from which that codeword was decoded, and the overall cost of that codeword.

More precisely, a constituent SCL decoder for $\text{RM}(r, m)$ with maximum output-list-size $\ell_{\max} \in \mathbb{Z}^{\geq 2}$ and input-list-size $\ell_{\text{in}} \leq \ell_{\max}$ is a function

$$\Xi_{r,m}^{\ell_{\text{in}}, \ell_{\max}} : (\overline{\mathbb{R}}^{2^m} \times \overline{\mathbb{R}})^{\ell_{\text{in}}} \rightarrow (\text{RM}(r, m) \times [\ell_{\text{in}}] \times \overline{\mathbb{R}})^{\ell_{\text{out}}},$$

where $\ell_{\text{out}} = \min(2^{k(r,m)} \ell_{\text{in}}, \ell_{\max})$. We will start by defining this function for the special case when $m = 0$, *i.e.*, for a leaf decoder.

When $m = 0$, the SCL decoder is a map

$$\Xi_{r,0}^{\ell_{\text{in}}, \ell_{\max}} : (\overline{\mathbb{R}} \times \overline{\mathbb{R}})^{\ell_{\text{in}}} \rightarrow (\text{RM}(r, 0) \times [\ell_{\text{in}}] \times \overline{\mathbb{R}})^{\ell_{\text{out}}},$$

where $\ell_{\text{out}} = \min(2^{k(r,0)}\ell_{\text{in}}, \ell_{\text{max}})$. Thus the input to a leaf decoder is a list of pairs $((\lambda_0, \psi_0), \dots, (\lambda_{\ell_{\text{in}}-1}, \psi_{\ell_{\text{in}}-1})) \in (\mathbb{R} \times \mathbb{R})^{\ell_{\text{in}}}$, where λ_i is an LLR value and ψ_i is the associated cost. Two cases must be considered:

- If $r \geq 0$, then $\text{RM}(r, 0) = \{\mathbf{0}_1, \mathbf{1}_1\}$. In this case, for each λ_i , $i \in [\ell_{\text{in}}]$, there are two possible codewords: $\mathbf{0}$ with overall cost $\psi_i + \mathcal{L}(\mathbf{0}, \lambda_i) = \psi_i + \eta(\lambda_i)$ leading to the tentative output triple $(\mathbf{0}, i, \psi_i + \eta(\lambda_i))$, and $\mathbf{1}$ with overall cost $\psi_i + \mathcal{L}(\mathbf{1}, \lambda_i) = \psi_i + \eta(-\lambda_i)$ leading to the tentative output triple $(\mathbf{1}, i, \psi_i + \eta(-\lambda_i))$. In total there will be $2\ell_{\text{in}}$ tentative output triples. If needed, this list of tentative triples is truncated to length ℓ_{max} , with the decoder returning only those candidates with the least overall cost.
- If $r < 0$, then $\text{RM}(r, 0) = \{\mathbf{0}_1\}$. In this case $\mathbf{0}$ is the only possible candidate codeword for each λ_i , $i \in [\ell_{\text{in}}]$, leading to output triple $(\mathbf{0}, i, \psi_i + \eta(\lambda_i))$. All ℓ_{in} of the resulting triples are returned by the decoder.

When $m > 0$, suppose the input to the SCL decoder is the ℓ_{in} -tuple

$$\boldsymbol{\tau} = \left(((\boldsymbol{\lambda}'_i | \boldsymbol{\lambda}''_i), s_i)_{i \in [\ell_{\text{in}}]} \right),$$

with $\boldsymbol{\lambda}'_i$ and $\boldsymbol{\lambda}''_i \in \overline{\mathbb{R}}^{2^{m-1}}$ and $s_i \in \overline{\mathbb{R}}$. We will then have

$$\Xi_{r,m}^{\ell_{\text{in}}, \ell_{\text{max}}}(\boldsymbol{\tau}) \triangleq \left(((\mathbf{u}_i | \mathbf{u}_i \oplus \mathbf{v}_i), p_{q_i}, s'_i)_{i \in [\ell_{\text{out}}]} \right) \quad (11)$$

where \mathbf{v}_j 's and the p_j 's in (11) are obtained from

$$\left((\mathbf{v}_j, p_j, s''_j)_{j \in [\ell']} \right) = \Xi_{r-1, m-1}^{\ell_{\text{in}}, \ell_{\text{max}}} \left(((\boldsymbol{\lambda}'_i \boxplus \boldsymbol{\lambda}''_i, s_i)_{i \in [\ell_{\text{in}}]} \right), \quad (12)$$

where

$$\ell' = \min(2^{k(r-1, m-1)}\ell_{\text{in}}, \ell_{\text{max}}). \quad (13)$$

Moreover, the \mathbf{u}_j 's, the q_j 's, and the s'_j 's in (11) are obtained from

$$\left((\mathbf{u}_j, q_j, s'_j)_{j \in [\ell'']} \right) = \Xi_{r, m-1}^{\ell', \ell_{\text{max}}} \left(((\boldsymbol{\lambda}'_{p_j} + (-1)^{\mathbf{v}_j} \boldsymbol{\lambda}''_{p_j}, s''_j)_{j \in [\ell']} \right), \quad (14)$$

where

$$\ell'' = \min(2^{k(r, m-1)}\ell', \ell_{\text{max}}) = \min(2^{k(r, m)}\ell_{\text{in}}, \ell_{\text{max}}). \quad (15)$$

The overall SCL decoder for $\text{RM}(r, m)$ is obtained by setting $\ell_{\text{in}} = 1$ and by choosing any arbitrary real number as the initial cost of its input LLR vector. The overall decoder returns the codeword having the smallest analog weight with respect to the input LLR vector from the list of candidates returned by the decoder at the root of the decoding tree.

F. AE Decoding of RM Codes

As described in Sec. I and as illustrated in Fig. 3, an AE decoder operates by permuting the received LLR vector $\boldsymbol{\lambda}$ by the elements of a set $\mathcal{E} = \{\pi_1, \dots, \pi_\ell\}$, called an *automorphism ensemble*, of code automorphisms. Each of the ℓ permuted LLR vectors is then decoded (perhaps in parallel) using a simple sub-optimal *elementary decoder* such as a GMC decoder, and the corresponding inverse permutation is applied to each decoding result. The most likely codeword is then selected from the ℓ generated candidates.

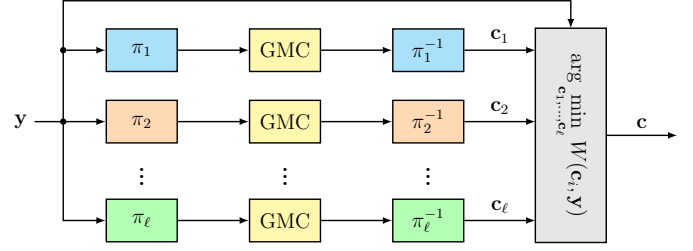


Fig. 3. The general architecture of an AE decoder corresponding to an automorphism ensemble of size ℓ .

For any choice of atom set \mathcal{A} and any automorphism $\pi \in \mathbb{A}_{r,m}$, let $L_{r,m}^{\pi, \mathcal{A}} : \overline{\mathbb{R}}^{2^m} \rightarrow \text{RM}(r, m)$ denote the π -permuted GMC decoder, defined as

$$L_{r,m}^{\pi, \mathcal{A}} \triangleq \pi^{-1} \circ \Gamma_{r,m}^{\mathcal{A}} \circ \pi, \quad (16)$$

where \circ denotes function composition. Thus $L_{r,m}^{\pi, \mathcal{A}}(\boldsymbol{\lambda}) = \pi^{-1} \Gamma_{r,m}^{\mathcal{A}}(\pi \boldsymbol{\lambda})$. Of course $L_{r,m}^{\text{id}, \mathcal{A}} = \Gamma_{r,m}^{\mathcal{A}}$, i.e., the id-permuted GMC decoder is just the GMC decoder itself.

Depending on the choice of π , because of the suboptimality of a GMC decoder, it may happen that

$$\Gamma_{r,m}^{\mathcal{A}} \neq L_{r,m}^{\pi, \mathcal{A}}. \quad (17)$$

This is useful, because if $\Gamma_{r,m}^{\mathcal{A}}$ makes an error, there is a possibility that $L_{r,m}^{\pi, \mathcal{A}}$ can nevertheless decode correctly, and *vice versa*. Automorphism ensemble decoding of RM codes [1], [11], [12] exploits (17) to decode a received LLR vector using an ensemble \mathcal{E} of automorphisms with the property, that

$$\pi_1, \pi_2 \in \mathcal{E}, \pi_1 \neq \pi_2 \text{ implies } L_{r,m}^{\pi_1, \mathcal{A}} \neq L_{r,m}^{\pi_2, \mathcal{A}}. \quad (18)$$

Indeed, if $L_{r,m}^{\pi_i, \mathcal{A}}$, $\pi_i \in \mathcal{E}$, produces decoding decision \mathbf{c}_i , then the overall AE decoding decision is given, as illustrated in Fig. 3, by

$$\mathbf{c} = \arg \min_{\mathbf{c}_1, \dots, \mathbf{c}_\ell} w(\mathbf{c}_i, \boldsymbol{\lambda}),$$

where the analog-weight function w was defined in (2).

III. CONSTITUENT AUTOMORPHISM DECODING

Like all successive-cancellation decoding schemes, GMC decoders are prone to error propagation: once a leaf decoder makes an error, the error propagates to all succeeding decoders encountered in the decoding tree traversal. Because of channel polarization [7], different constituent leaf decoders of an RM code observe different synthetic channels and, as a result, they have different *first-error probability*, the probability that they produce an error while all preceding leaf decoders have decoded correctly. For example, Table I gives the binary addresses of the leaf constituent codes of $\Gamma_{4,9}^{\mathcal{A}}$ having the largest first-error probability at the output of a BI-AWGN channel with an SNR of 4 dB. It is clear that most decoding errors are triggered by the leaf decoder with address 111.

Because of this channel polarization effect, it is sensible to devote more decoding resources to those constituent codes having relatively degraded channels, as these trigger the most decoding errors. However, a conventional AE decoder treats all constituent codes evenly. In particular, via an AE decoder

TABLE I
LEAVES WITH LARGEST FIRST-ERROR PROBABILITY IN $\Gamma_{4,9}^{\mathcal{A}^*}$.

address	contribution	address	contribution
111	91.6%	1101	7.39%
11001	0.5%	1011	0.4%

(BI-AWGN channel, SNR=4dB)

with some automorphism ensemble \mathcal{E} , each constituent code of a composite RM code is decoded $|\mathcal{E}|$ times. To remedy this issue, we introduce constituent automorphism decoding. The key idea is to apply AE decoding *locally* to the codes that are composite with respect to a given atom set \mathcal{A} .

With a random selection of \mathcal{E} from $\mathbb{A}_{r,m}$ chosen to satisfy (18), we did not see any difference in BLER at the output of a BI-AWGN between various selected automorphism ensembles for any of the $\text{RM}(r,m)$ codes that we tested. Thus we speculate that the performance of an AE decoder depends only on the ensemble size. As a result, we will only specify the AE size, without describing the actual automorphisms used.

By default, all decoders in the decoding tree will use an AE size of one (conveniently implemented with an automorphism ensemble containing just the identity permutation id). However, certain selected composite (non-leaf) decoders will use AE decoding locally with a larger AE size.

To specify the local decoders having an AE size greater than unity, we define an *automorphism distribution* \mathcal{S} as a set of (\mathbf{a}, s) pairs, where \mathbf{a} is the binary address of a decoder in $\mathbb{T}_{r,m}^{\mathcal{A}}$ and s is the corresponding AE size. For example, $\mathcal{S} = \{(1, 2), (11, 3)\}$ denotes a CA decoder that applies AE decoding with AE size 2 at the decoding tree vertex with address 1, and AE decoding with AE size 3 at the vertex with address 11. In this notation, a conventional AE decoder with AE size s has automorphism distribution $\mathcal{S} = \{(\emptyset, s)\}$. We denote the CA decoder for $\text{RM}(r,m)$ with automorphism distribution \mathcal{S} and atom set \mathcal{A} as

$$\Psi_{r,m}^{\mathcal{S},\mathcal{A}} : \mathbb{R}^{2^m} \rightarrow \text{RM}(r,m).$$

In the rest of this paper, all CA decoders use the atom set \mathcal{A}^* . The leaf decoders associated with \mathcal{A}^* are permutation invariant ML decoders, so applying AE to them cannot improve performance. Hence the AE size of leaf nodes in $\mathbb{T}_{r,m}^{\mathcal{A}^*}$ is fixed to unity. As we will show in Sec. V, most of the benefit of CA decoding arises when the addresses \mathbf{a} are chosen from the set $\{\emptyset, 1, 11, 111, \dots\}$ which are called *rightmost nodes*, as these correspond to the synthetic channels that polarize to relatively “bad” channels. A slightly better heuristic for choosing the vertices at which to apply AE decoding is given in Sec. V-A.

IV. COMPLEXITY ANALYSIS

A. Basic Operations

It is difficult to give a precise analysis of decoding complexity, as it strongly depends on the available hardware and its architecture. Nevertheless, complexity (measured by the area-time product of an integrated circuit implementation, or in execution time of a software implementation) will scale approximately linearly with the number of unary and binary

operations executed by the decoding algorithm. Accordingly, we will measure complexity by counting such operations (in the worst case) for each of the decoders that we consider.

In practice, LLR values are often represented using a fixed point (integer) representation with a fixed word size. We will assume that vectors of length n , whether integer- or \mathbb{F}_2 -valued, are stored as sequences of n words. All decoders that we consider are implemented as sequences of the following basic unary and binary operations (operating on one or two words): addition (+), comparison (<, >, ≤, ≥), minimum and maximum (min, max), soft XOR (\boxplus), negative log-sigmoid (η), absolute value ($|\cdot|$), negation (−), binary addition (\oplus), and, finally, copying a word or its negation.

We assume the soft XOR and the negative log-sigmoid operations are calculated by look-up tables or hardware-friendly approximations. In a pipelined processor architecture, the fetching of operands and the storing of results take place in parallel with instruction decoding and execution, so we do not assign additional complexity for such operations. Assuming the use of pipelining, all of these basic operations can be executed in a single clock cycle on average. Accordingly, we weight these operations evenly, taking their total count χ as a measure of decoder complexity.

Let $D_{r,m}$ denote a decoder for $\text{RM}(r,m)$ and let $\chi_D(r,m)$ denote its complexity. Except at leaf decoders, $D_{r,m}$ is defined recursively in terms of $D_{r-1,m-1}$ and $D_{r,m-1}$, the decoders for its Plotkin constituents. Depending on the nature of the decoder, these constituent decoders may be invoked more than once. It follows that $\chi_D(r,m)$ will generally decompose (recursively) into three terms: i) a term that accounts for one or more applications of $D_{r-1,m-1}$, ii) a term that accounts for one or more applications of $D_{r,m-1}$, and iii) a term that accounts for the preparation of LLRs and the final decision. Leaf decoders are *not* defined recursively, and thus each such decoder will require its own separate complexity analysis.

B. Complexity of CA, GMC, and AE decoders

For all nontrivial RM codes, assuming use of the atom set \mathcal{A}^* defined in (8), the only required leaf decoders are those for the $\text{RM}(m-1,m)$ SPC codes and $\text{RM}(1,m)$ first-order RM codes.

1) $\text{RM}(m-1,m)$: The worst-case complexity of applying the Wagner decoding rule to the $\text{RM}(m-1,m)$ SPC code can be separated into:

- converting LLRs to hard-decisions, which requires 2^m comparisons;
- determining the overall parity, which requires $2^m - 1$ binary field additions;
- checking whether the overall parity is nonzero, which requires 1 comparison,
- flipping the bit with the least absolute LLR value (if the parity bit is nonzero), which requires 2^m absolute value computations, $2^m - 1$ comparisons, and 1 binary field addition.

Adding these values gives

$$\chi(m-1,m) = 2^{m+2}. \quad (19)$$

Algorithm 1 Map sign and index to $\mathbf{v} \in \text{RM}(1, m)$.

Require: $m \in \mathbb{Z}^{\geq 0}$, sign $s \in \mathbb{F}_2$, index vector $\mathbf{i} \in \mathbb{F}_2^m$

```

1:  $\mathbf{v} \leftarrow (s)$ 
2: for  $j \in [m]$  do
3:   if  $\mathbf{i}[m-1-j] = 0$  then
4:      $\mathbf{v} \leftarrow (\mathbf{v} \mid \mathbf{v})$  ▷ ( $2^j$  copy operations.)
5:   else
6:      $\mathbf{v} \leftarrow (\mathbf{v} \mid \bar{\mathbf{v}})$  ▷ ( $2^j$  negated-copy operations.)
7:   end if
8: end for
9: return  $\mathbf{v}$ 

```

Remarks: For each $j \in [m]$, executing line 4 or 6 requires 2^j copy or negated-copy operations. Neglecting loop overhead, we have one initial copy of the sign bit, 1 comparison per loop (for a total of m comparisons) and $\sum_{i=0}^{m-1} 2^i = 2^m - 1$ copy operations, yielding a total complexity of $2^m + m$ operations.

2) $\text{RM}(1, m)$: The worst-case complexity of decoding $\text{RM}(1, m)$, the length- 2^m first-order RM code, using the Green Machine decoder can be separated into:

- applying the fast Hadamard transform to the given LLR vector, which requires $m \cdot 2^m$ additions;
- finding the index with the largest absolute value, which requires 2^m absolute value computations, and $2^m - 1$ comparisons;
- extracting the sign of the corresponding LLR, which requires 1 comparison,
- converting the sign and index to a codeword, which requires $2^m + m$ operations according to Algorithm 1.

Adding these values gives

$$\chi(1, m) = (m + 3)2^m + m. \quad (20)$$

Let $\chi_{\Psi}(r, m, \mathcal{S})$ denote the complexity of $\Psi_{r, m}^{\mathcal{S}, \mathcal{A}^*}$, the CA decoder for a composite $\text{RM}(r, m)$ under an automorphism distribution \mathcal{S} and with atom set \mathcal{A}^* . Let ℓ denote the number of automorphisms applied at the root of the decoding tree. Note that $(\emptyset, \ell) \in \mathcal{S}$ if and only if $\ell > 1$. A CA decoder for $\text{RM}(r, m)$ using \mathcal{S} invokes CA decoders for the Plotkin constituents of the code, *i.e.*, $\text{RM}(r-1, m-1)$ and $\text{RM}(r, m-1)$, using, respectively, the automorphism distributions \mathcal{S}_1 and \mathcal{S}_0 , defined as

$$\begin{aligned} \mathcal{S}_1 &\triangleq \{(\mathbf{a}, s_{\mathbf{a}}) : ((1 \mid \mathbf{a}), s_{\mathbf{a}}) \in \mathcal{S}\} \text{ and} \\ \mathcal{S}_0 &\triangleq \{(\mathbf{a}, s_{\mathbf{a}}) : ((0 \mid \mathbf{a}), s_{\mathbf{a}}) \in \mathcal{S}\}. \end{aligned}$$

The number of operations contributing to $\chi_{\Psi}(r, m, \mathcal{S})$ decomposes as follows:

- preparing LLRs for $\Psi_{r-1, m-1}^{\mathcal{S}_1, \mathcal{A}^*}$ in accordance with (6), which requires $\ell 2^{m-1}$ soft XOR operations;
- invoking ℓ instances of $\Psi_{r-1, m-1}^{\mathcal{S}_1, \mathcal{A}^*}$, which requires $\ell \chi_{\Psi}(r-1, m-1, \mathcal{S}_1)$ operations;
- preparing LLRs for $\Psi_{r, m-1}^{\mathcal{S}_0, \mathcal{A}^*}$ in accordance with (7), which requires $\ell 2^{m-1}$ comparisons and $\ell 2^{m-1}$ additions;
- invoking ℓ instances of $\Psi_{r, m-1}^{\mathcal{S}_0, \mathcal{A}^*}$, which requires $\ell \chi_{\Psi}(r, m-1, \mathcal{S}_0)$ operations;
- combining Plotkin constituents according to (5), which requires $\ell 2^{m-1}$ binary field additions;

- choosing the codeword with minimum analog weight among ℓ candidates, which if $\ell = 1$ requires no operations and if $\ell > 1$ requires $\ell 2^m$ comparisons and $\ell(2^m - 1)$ additions for computing analog weight, and another $\ell - 1$ comparisons for choosing the final codeword.

As a result,

$$\chi_{\Psi}(r, m, \mathcal{S}) = \ell \chi_{\Psi}(r-1, m-1, \mathcal{S}_1) + \ell \chi_{\Psi}(r, m-1, \mathcal{S}_0) + \ell 2^{m+1} + \mathbb{1}_{\ell > 1} \cdot (\ell 2^{m+1} - 1),$$

with boundary conditions $\chi_{\Psi}(m-1, m, \{\}) = \chi(m-1, m)$ and $\chi_{\Psi}(1, m, \{\}) = \chi(1, m)$, defined in (19) and (20), respectively.

GMC and AE decoders are special cases of a CA decoder and so their complexity may be expressed in terms of χ_{Ψ} . Since all nodes in the decoding tree of a GMC decoder use only the identity automorphism, the automorphism distribution for such a decoder is $\mathcal{S} = \{\}$; thus

$$\chi_{\text{GMC}}(r, m) = \chi_{\Psi}(r, m, \{\}). \quad (21)$$

An AE decoder with an automorphism ensemble of size ℓ has automorphism distribution $\mathcal{S} = \{(\emptyset, \ell)\}$; thus,

$$\chi_{\text{AE}}(r, m, \ell) = \chi_{\Psi}(r, m, \{(\emptyset, \ell)\}). \quad (22)$$

C. Complexity of SCL Decoders

We assume that $\text{RM}(r, m)$ has a non-negative order and that the atom set \mathcal{A}' is used. Similar to CA decoders, we first discuss the complexity of list decoding of codes in \mathcal{A}' . We then derive the complexity of the SCL decoder for a composite code $\text{RM}(r, m)$.

1) $\text{RM}(r, m) \in \mathcal{A}'$: For list-truncation purposes, some of the leaf SCL decoders must find the least ℓ_{\max} numbers among an unsorted list of n numbers, where $n \in \mathbb{Z}$. When $\ell_{\max} < n$, there are a number of algorithms for this task, each having its own complexity. We denote by $\chi_{\text{sel}}(\ell_{\max}, n)$ the number of basic operations required for this task in the worst case. Clearly $\chi_{\text{sel}}(\ell_{\max}, n) = 0$ when $\ell_{\max} \geq n$.

In this paper, we use (ℓ_{\max}, n) *selection networks*, which combine a fixed number of *comparator* and *minimum selector* (minselector) elements to achieve a deterministic number of basic operations for selection of the smallest ℓ_{\max} entries from an input list of size $n > \ell_{\max}$ [21, Sec. 5.3.4], [22]. A comparator is a two-input two-output computational unit, that transforms a pair (x, y) of input scores to $(\min(x, y), \max(x, y))$, requiring two basic operations. Similarly, a minselector is a two-input one-output unit, transforming a pair (x, y) to $\min(x, y)$, requiring one basic operation. Since $n - \ell_{\max}$ inputs are dropped by an (ℓ_{\max}, n) selection network, the number of minselectors in such a network will always be $n - \ell_{\max}$. Thus, an (ℓ_{\max}, n) selection network with a total of T computational units (comparators and minselectors) requires $\chi_{\text{sel}}(\ell_{\max}, n) = 2T - (n - \ell_{\max})$ basic operations.

An (ℓ_{\max}, n) selection network is said to be *optimal* if the total number T of computational units that it contains is as small as possible; this minimum possible number of computational units is denoted as $U_{\ell_{\max}}(n)$. The exact value

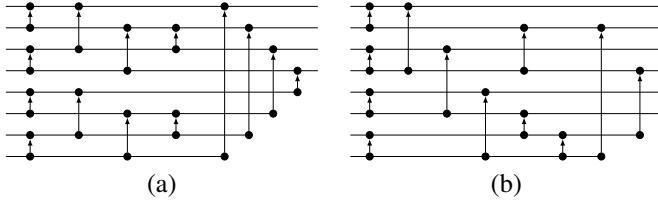


Fig. 4. Selection networks with parameters: (a) (4,8), (b) (6,8). Vertical segments denote comparators (having two output ports) and miniselectors (having one output port), with an arrow pointing towards the output port corresponding to the minimum input.

of $U_{\ell_{\max}}(n)$ is known only for small values of ℓ_{\max} and n ; however, it is known that [21, Sec. 5.3.4, Thm. A]

$$U_{\ell_{\max}}(n) \geq (n - \ell_{\max}) \lceil \log_2(\ell_{\max} + 1) \rceil. \quad (23)$$

Fig. 4 shows conjectured-optimal (4,8) and optimal (6,8) selection networks.

Table II shows the value for $\chi_{\text{sel}}(\ell_{\max}, n)$ for different values of ℓ_{\max} and n encountered in SCL decoding of RM codes in Sec. V. The values for $\chi_{\text{sel}}(4, 8)$ and $\chi_{\text{sel}}(6, 8)$ correspond to the selection networks of Fig. 4. In the (6, 12) case, we have assumed that the lower bound in (23) is achieved with equality; however, in practice this bound may not be achievable, and thus $\chi_{\text{sel}}(6, 12)$ may be larger than the value given in the table.

Let $\chi_{\Xi}(r, m, \ell_{\text{in}}, \ell_{\text{max}})$ denote the decoding complexity of $\Xi_{r,m}^{\ell_{\text{in}}, \ell_{\text{max}}}$. We start by considering $\chi_{\Xi}(r, 0, \ell_{\text{in}}, \ell_{\text{max}})$, i.e., the decoding complexity of the leaf decoders $\Xi_{r,0}^{\ell_{\text{in}}, \ell_{\text{max}}}$.

For an input-list size $\ell_{\text{in}} \in \mathbb{Z}^{\geq 1}$ and a maximum output-list size $\ell_{\text{max}} \in \mathbb{Z}^{\geq 2}$, the complexity of applying $\Xi_{r,0}^{\ell_{\text{in}}, \ell_{\text{max}}}$ to decode LLR values $\lambda_0, \dots, \lambda_{\ell_{\text{in}}-1}$ to a codeword (of length one) in $\text{RM}(r, 0)$ can be separated into the following steps.

- Computing the overall cost of each tentative candidate codeword along with the value of that codeword. For the zero codeword this requires one call to η , one addition, and one bit-copy operation, for a total cost of $3\ell_{\text{in}}$ basic operations. When $r \geq 0$, the nonzero codeword requires these operations and an extra negation for an additional cost of $4\ell_{\text{in}}$ basic operations. In total, this results in $\ell_{\text{in}}(3 + 4 \cdot \mathbb{1}_{r \geq 0})$ operations.
- Finding the (at most) ℓ_{max} codewords having least cost from a list of $2^{k(r,0)}\ell_{\text{in}}$ codewords, which requires $\chi_{\text{sel}}(\ell_{\text{max}}, 2^{k(r,0)}\ell_{\text{in}})$ basic operations.

Adding the number of basic operations for these steps gives

$$\chi_{\Xi}(r, 0, \ell_{\text{in}}, \ell_{\text{max}}) = \ell_{\text{in}}(3 + 4 \cdot \mathbb{1}_{r \geq 0}) + \chi_{\text{sel}}(\ell_{\text{max}}, 2^{k(r,0)}\ell_{\text{in}}). \quad (24)$$

2) $\text{RM}(r, m) \notin \mathcal{A}'$: For an input-list size ℓ_{in} and a maximum output-list size ℓ_{max} , the complexity of applying $\Xi_{r,m}^{\ell_{\text{in}}, \ell_{\text{max}}}$ to decode $\text{RM}(r, m) \notin \mathcal{A}'$ decomposes as follows:

TABLE II
VALUES FOR $\chi_{\text{SEL}}(\ell_{\text{max}}, n)$

ℓ_{max}, n	χ_{sel}	ℓ_{max}, n	χ_{sel}	ℓ_{max}, n	χ_{sel}
4,8	24	6,8	22	6,12	30

- preparing LLRs for $\Xi_{r-1, m-1}^{\ell_{\text{in}}, \ell_{\text{max}}}$ in accordance with (12), which requires $\ell_{\text{in}}2^{m-1}$ soft XOR operations;
- invoking $\Xi_{r-1, m-1}^{\ell_{\text{in}}, \ell_{\text{max}}}$, which requires $\chi_{\Xi}(r-1, m-1, \ell_{\text{in}}, \ell_{\text{max}})$ operations;
- preparing LLRs in accordance with (14), which requires $\ell'2^{m-1}$ comparisons and $\ell'2^{m-1}$ additions where ℓ' is given in (13);
- invoking $\Xi_{r, m-1}^{\ell', \ell_{\text{max}}}$, which requires $\chi_{\Xi}(r, m-1, \ell', \ell_{\text{max}})$ operations;
- combining Plotkin constituents, which requires $\ell''2^{m-1}$ binary field additions where ℓ'' is as (15).

As a result,

$$\chi_{\Xi}(r, m, \ell_{\text{in}}, \ell_{\text{max}}) = \chi_{\Xi}(r-1, m-1, \ell_{\text{in}}, \ell_{\text{max}}) + \chi_{\Xi}(r, m-1, \ell', \ell_{\text{max}}) + 2^{m-1}(\ell_{\text{in}} + 2\ell' + \ell''), \quad (25)$$

with boundary conditions defined by leaf decoders according to (24). The complexity of the overall SCL decoder with a maximum output-list size of ℓ_{max} is then $\chi_{\Xi}(r, m, 1, \ell_{\text{max}})$.

V. NUMERICAL RESULTS

In this section, using numerical simulations we provide performance versus complexity and BLER versus SNR trade-offs for the schemes described in this paper. We assume transmission over a BI-AWGN channel. Performance is measured by the gap to the constrained Shannon limit at a BLER of 10^{-3} . Complexity is measured as the worst-case number of operations, computed according to Sec. IV, normalized by the code dimension.

A. Selection of automorphism distribution

There are numerous possible ways to choose an automorphism distribution. It is an open problem to determine the automorphism distribution that leads to the best performance at a given decoding complexity. Guided by the following numerical results, we provide a heuristic method for finding “good” CA decoders.

We first compare the performance-complexity tradeoffs of CA decoders for $\text{RM}(4, 9)$ for a large number of different choices of automorphism distribution. According to Table I, most decoding errors are caused by rightmost leaf decoders. We have tested addresses in automorphism distributions involving the first 5 nodes in the reverse pre-order decoding tree traversal (namely, nodes with address $\emptyset, 1, 11, 110$, and 1100), with AE size for each address ranging from 1 to 4. The results are given in Fig. 5.

The lower hull in Fig. 5 is the *Pareto frontier*; it connects the *Pareto-efficient points*. A point is Pareto-efficient with respect to a given set of points if no other point in the set can achieve better performance with the same or lower complexity. The parameters of the Pareto-efficient points in this test are given in Table III.

We categorize the tested automorphism distributions in Fig. 5 into four classes: (a) no rightmost nodes, (b) only root node, (c) only rightmost nodes (excluding only root node), (d) others. It is clear that CA decoders in class (a) have almost the same decoding performance as the GMC decoder,

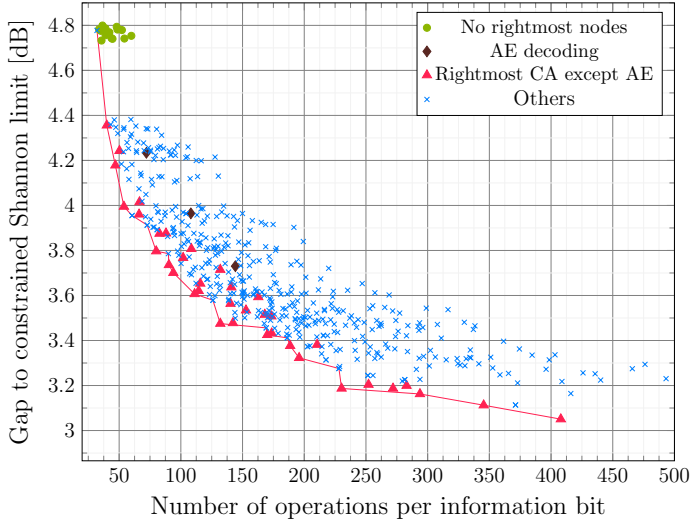


Fig. 5. An extensive test of CA decoders of RM(4,9) at BLER= 10^{-3} . Candidates nodes are those with address in the set $\{\emptyset, 1, 11, 110, 1100\}$ with ensemble size for each candidate node ranging from 1 to 4.

TABLE III
PARETO-EFFICIENT POINTS IN FIG. 5.

Decoder	Operations per information bit	Gap to CSL
GMC	32.043	4.778
(11, 2)	39.984	4.356
(11, 3)	46.93	4.178
(11, 4)	53.875	3.995
(11, 4); (1100, 2)	60.469	3.955
(1, 2); (11, 2); (1100, 2)	72.734	3.913
(1, 2); (11, 3)	80.031	3.797
(1, 2); (11, 3); (1100, 2)	89.922	3.786
(1, 3); (11, 2)	90.301	3.736
(1, 2); (11, 4)	93.922	3.701
(1, 3); (11, 3)	111.137	3.607
(1, 3); (11, 3); (1100, 2)	125.973	3.579
(1, 3); (11, 4)	131.973	3.475
(1, 4); (11, 2); (110, 3)	169.18	3.456
(1, 4); (11, 4)	170.023	3.425
(1, 4); (11, 3); (110, 2)	186.258	3.412
(\emptyset , 2); (1, 3); (11, 2)	188.598	3.376
(\emptyset , 2); (1, 2); (11, 4)	195.84	3.323
(\emptyset , 2); (1, 4); (110, 3)	228.105	3.276
(\emptyset , 2); (1, 3); (11, 3)	230.27	3.187
(\emptyset , 3); (1, 2); (11, 4)	293.762	3.162
(\emptyset , 3); (1, 3); (11, 3)	345.406	3.113
(\emptyset , 3); (1, 3); (11, 4)	407.914	3.051

which implies that including the rightmost nodes is a necessary condition to make an improvement. The Pareto frontier has roughly 0.2 dB gain from decoders in (b), which shows the advantage of CA decoding compared to AE decoding. CA decoders with automorphism distributions satisfying (c) are called *rightmost* CA decoders. According to Fig. 5 and Table III, the Pareto-efficient points involve automorphism distributions where only rightmost or “nearly rightmost” vertices in the decoding tree receives an AE size greater than one.

These observations suggest the following heuristic method for choosing an automorphism distribution where only rightmost composite decoders (*i.e.*, the root or any non-leaf decoder with an all-ones address) receive an AE size greater than unity. Let $m(i)$ denote the AE size for the right-most composite

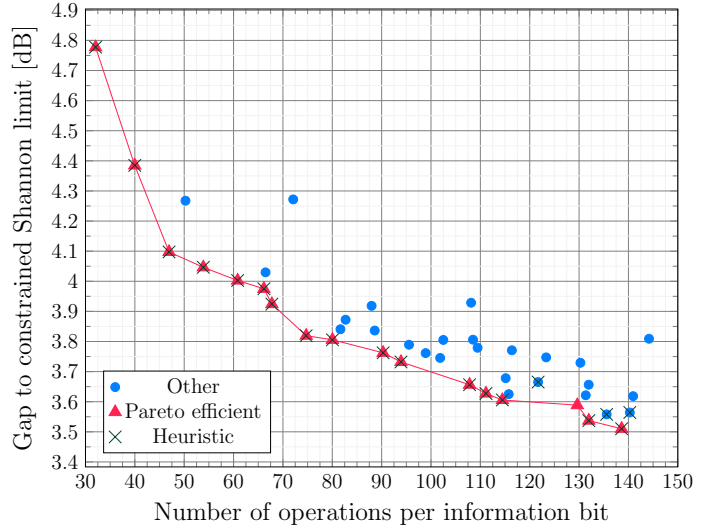


Fig. 6. CA decoders for code RM(4,9) at BLER= 10^{-3} having complexity no more than AE-4.

TABLE IV
PARETO-EFFICIENT POINTS IN FIG. 6.

Decoder	Operations per information bit	Gap to CSL
GMC	32.043	4.778
(11, 2)	39.984	4.385
(11, 3)	46.93	4.097
(11, 4)	53.875	4.046
(11, 5)	60.82	4.003
(1, 2); (11, 2)	66.141	3.975
(11, 6)	67.766	3.924
(11, 7)	74.711	3.819
(1, 2); (11, 3)	80.031	3.806
(1, 3); (11, 2)	90.301	3.762
(1, 2); (11, 4)	93.922	3.732
(1, 2); (11, 5)	107.812	3.656
(1, 3); (11, 3)	111.137	3.627
(1, 4); (11, 2)	114.461	3.606
(\emptyset , 2); (11, 5)	129.637	3.589
(1, 3); (11, 4)	131.973	3.537
(1, 5); (11, 2)	138.621	3.51

decoder at depth i in $\mathbb{T}_{r,m}^{A*}$. The heuristic would then choose:

- 1) $m(i) \leq 7$ for all i , *i.e.*, the number of automorphisms applied at any local decoder is restricted; and
- 2) if $m(i) \geq 2$ then $m(j) \geq 2$ for all $j \geq i$, *i.e.*, AE decoding with size greater than unity should be applied at a node only when all of its right descendants also have AE size greater than unity.

Fig. 6 shows the performance of all decoders for RM(4,9), where AE decoding is applied at the right-most composite decoders. Included are those decoders whose complexity does not exceed that of AE-4, *i.e.*, the CA decoder with $\mathcal{S} = \{(\emptyset, 4)\}$. It can be seen that almost all Pareto-efficient points are selected by the given heuristic and all heuristically chosen decoders are close to the Pareto frontier (within 0.07 dB). The decoder parameters for Pareto-efficient points in Fig. 6 are given in Table IV.

In the following comparisons, the CA decoders were all selected using the heuristic described above.

TABLE V
DECODING COMPLEXITY FOR RM CODES OF RATE 1/2 IN FIG. 7.

Code	Decoder	Operations per information bit
RM(3, 7)	GMC	25.10
	SCL-6	225.80
	AE-6	174.55
	$(\emptyset, 4), (1, 2)$	175.05
RM(4, 9)	GMC	32.04
	SCL-4	195.47
	AE-4	144.17
	$(1, 4), (11, 3)$	142.24
RM(5, 11)	GMC	39.15
	SCL-4	230.31
	AE-4	172.6
	$(1, 2), (11, 2), (111, 6)$	157.41

B. Comparison of Decoders

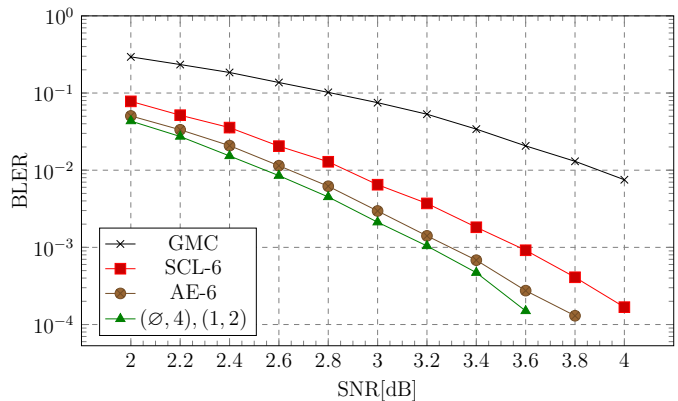
Fig. 7 compares the performance achieved by different decoders for three different RM codes of rate 1/2. Table V lists the complexity for each tested decoder. The AE, CA and SCL decoders that we have tested are approximately at the same complexity level. It is clear that the CA decoding algorithm outperforms the other decoders at the same complexity level.

Comparing the performance of CA and AE decoding, we find that the improvement changes for different codes. The improvement for RM(3, 7) is merely 0.1 dB, whereas there is a gain of 0.4 dB for RM(5, 11).

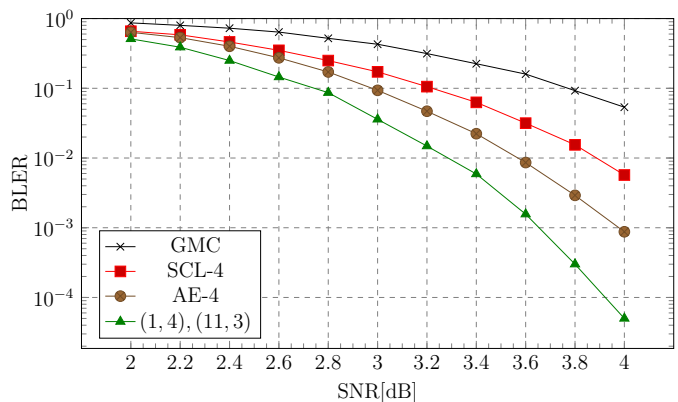
Fig. 8 shows a comparison of CA decoders and AE decoders for different RM codes with the same block length (same m). The Pareto-efficient CA decoders with decoding complexity not exceeding that of AE-4 are depicted with solid marks, while the AE decoders are drawn in hollow marks. We observe that the gap between the AE decoder and the CA decoder is larger for higher order r . In other words, the gain achieved when applying CA decoding compared to AE decoding is more significant for high order RM codes. This trend is expected, since higher order RM codes have more rightmost nodes, which means there are more nodes observing “bad” channel polarization, and therefore such codes benefit more from an uneven distribution of decoding resources.

VI. CONCLUSIONS

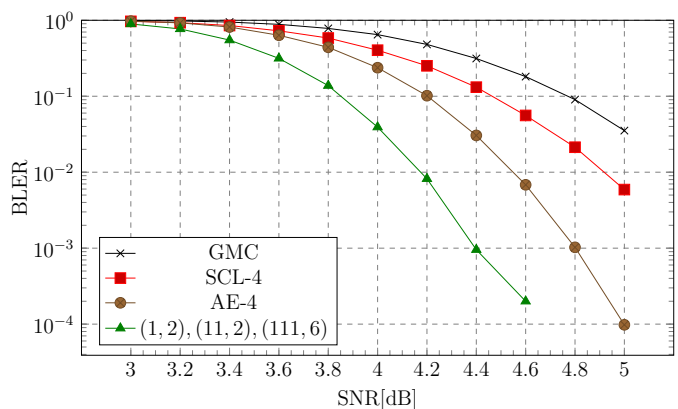
This paper has introduced the constituent automorphism (CA) decoding algorithm for RM codes, which applies AE decoding at the (mainly rightmost) constituent decoders according to a specified automorphism distribution. CA decoders can achieve better performance versus complexity trade-offs than other state-of-the-art decoding algorithms. The benefits of CA decoding appear to increase as the order of the RM code increases. While the problem of selecting an automorphism distribution achieving the best performance at a fixed complexity remains open, we have provided a simple heuristic by which a “good” automorphism distribution may be selected. In the future, it would be interesting to study whether CA decoding can be adapted to a suitable class of polar codes. As in [23], the chosen polar-code class would need to overcome the property that polar codes do not generally have a large automorphism group [24].



(a)



(b)



(c)

Fig. 7. Performance of decoders for RM codes of rate 1/2: (a) RM(3, 7), (b) RM(4, 9), and (c) RM(5, 11).

REFERENCES

- [1] M. Geiselhart, A. Elkelesh, M. Ebada, S. Cammerer, and S. ten Brink, “Automorphism ensemble decoding of Reed–Muller codes,” *IEEE Trans. Commun.*, vol. 69, no. 10, pp. 6424–6438, Oct. 2021.
- [2] I. Dumer and K. Shabunov, “Soft-decision decoding of Reed-Muller codes: recursive lists,” *IEEE Trans. Inf. Theory*, vol. 52, no. 3, pp. 1260–1266, 2006.
- [3] D. E. Muller, “Application of Boolean algebra to switching circuit design and to error detection,” *Trans. IRE Prof. Group Electron. Comput.*, vol. EC-3, no. 3, pp. 6–12, 1954.
- [4] I. Reed, “A class of multiple-error-correcting codes and the decoding scheme,” *Trans. IRE Prof. Group Inf. Theory*, vol. 4, no. 4, pp. 38–49, 1954.

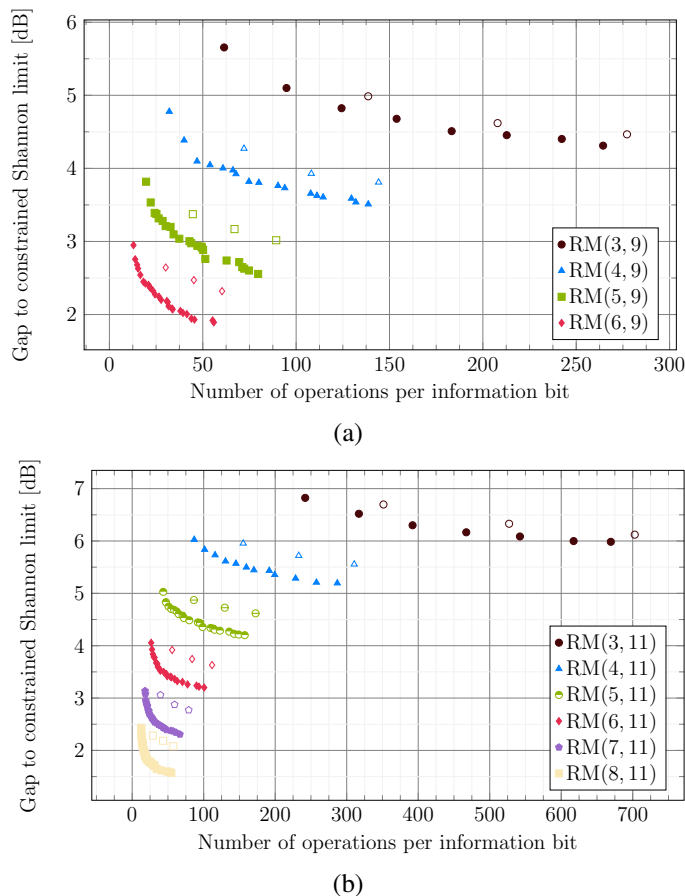


Fig. 8. Performance of RM codes with the same m (a) $m = 9$, (b) $m = 11$.

- [5] E. Abbe, O. Sberlo, A. Shpilka, and M. Ye, "Reed-Muller codes," *Foundations & Trends in Commun. & Inf. Theory*, vol. 20, no. 1–2, pp. 1–156, 2023.
- [6] G. Schnabl and M. Bossert, "Soft-decision decoding of Reed-Muller codes as generalized multiple concatenated codes," *IEEE Trans. Inf. Theory*, vol. 41, no. 1, pp. 304–308, 1995.

- [7] E. Arkan, "Channel polarization: A method for constructing capacity-achieving codes for symmetric binary-input memoryless channels," *IEEE Trans. Inf. Theory*, vol. 55, no. 7, pp. 3051–3073, 2009.
- [8] I. Tal and A. Vardy, "List decoding of polar codes," *IEEE Trans. Inf. Theory*, vol. 61, no. 5, pp. 2213–2226, 2015.
- [9] E. Prange, "The use of information sets in decoding cyclic codes," *IRE Trans. Inf. Theory*, vol. 8, no. 5, pp. 5–9, Sep. 1962.
- [10] F. J. Macwilliams, "Permutation decoding of systematic codes," *Bell Sys. Techn. J.*, vol. 43, no. 1, pp. 485–505, 1964.
- [11] M. Kameney, Y. Kameney, O. Kurmaev, and A. Maevskiy, "A new permutation decoding method for Reed-Muller codes," in *Int. Symp. Inf. Theory (ISIT)*, Paris, France, Jul. 2019, pp. 26–30.
- [12] K. Ivanov and R. Urbanke, "Permutation-based decoding of Reed-Muller codes in binary erasure channel," in *Int. Symp. Inf. Theory (ISIT)*, Paris, France, Jul. 2019, pp. 21–25.
- [13] C. Kestel, M. Geiselhart, L. Johannsen, S. ten Brink, and N. Wehn, "Automorphism ensemble polar code decoders for 6G URLLC," in *13th VDE Conf. on Sys., Commun., and Coding*, Braunschweig, Germany, Feb. 2023, pp. 1–6.
- [14] F. J. Macwilliams and N. J. A. Sloane, *The Theory of Error-Correcting Codes*. North-Holland Pub., 1977.
- [15] M. Plotkin, "Binary codes with specified minimum distance," *IRE Trans. Inf. Theory*, vol. 6, no. 4, pp. 445–450, 1960.
- [16] G. D. Forney, Jr., "Coset codes II: Binary lattices and related codes," *IEEE Trans. Inf. Theory*, vol. 34, no. 5, pp. 1152–1187, Sep. 1988.
- [17] R. A. Silverman and M. Balser, "Coding for constant-data-rate systems-part I. A new error-correcting code," *Proc. IRE*, vol. 42, no. 9, pp. 1428–1435, 1954.
- [18] Y. Be'ery and J. Snyders, "Optimal soft decision block decoders based on fast Hadamard transform," *IEEE Trans. Inf. Theory*, vol. 32, no. 3, pp. 355–364, 1986.
- [19] I. Dumer, "Soft-decision decoding of Reed-Muller codes: a simplified algorithm," *IEEE Trans. Inf. Theory*, vol. 52, no. 3, pp. 954–963, 2006.
- [20] A. Balatsoukas-Stimming, M. B. Parizi, and A. Burg, "LLR-based successive cancellation list decoding of polar codes," *IEEE Trans. Signal Process.*, vol. 63, no. 19, pp. 5165–5179, 2015.
- [21] D. E. Knuth, *The Art of Computer Programming*. Upper Saddle River, NJ: Addison-Wesley, 1998, vol. 3.
- [22] A. C.-C. Yao, "A study of concrete computational complexity," Ph.D. dissertation, University of Illinois at Urbana-Champaign, Urbana, IL, USA, May 1975.
- [23] C. Pillet, V. Bioglio, and I. Land, "Polar codes for automorphism ensemble decoding," in *IEEE Inf. Theory Workshop (ITW)*, Kanazawa, Japan (virtual), Oct. 2021, pp. 1–6.
- [24] K. Ivanov and R. Urbanke, "Polar codes do not have many affine automorphisms," in *Int. Symp. Inf. Theory (ISIT)*, Espoo, Finland, Jun. 2022, pp. 2374–2378.